

FMCW SIGNAL PROCESSING

Belinda J. Lipa and Donald E. Barrick
Mirage Systems, Sunnyvale, California

INTRODUCTION

In a conventional "pulse-Doppler" radar, a short pulse emitted by the radar is reflected from a target; the time delay and Doppler shift in the reflected signal are then used to deduce unambiguously the distance and velocity of the target. In a frequency-modulated continuous-wave (FMCW) radar, both transmitter and receiver are left on for extended periods and optimum processing leads to estimates of range and velocity with greatly improved signal-to-noise ratio. FMCW signal processing was treated by Barrick (1973). The purpose of this note is to provide more detail and extend the analysis to apply to a gated signal. The techniques are illustrated by the design of a system for detection of hard moving targets, with simulation and interpretation of the output.

Analysis methods for an FMCW system are given in Section 1; approximations are listed and the resulting biases estimated. These methods are extended to apply to gated signals in Section 2. In Section 3, these methods are applied in the design of a detection radar; Section 4 describes the simulation of the output in the presence of realistic noise. Finally, in Section 5, we discuss methods for the interpretation of the spectrum. To assist the reader, a list of symbols is included in the Appendix.

SECTION 1: ANALYSIS FOR CONTINUOUS WAVE SIGNAL

Form of the transmitted and received signals

The transmitted frequency has the structure shown in Fig. 1, with the frequency increasing linearly as a function of time over the sweep period. The frequency at time t within each sweep is given by

$$f = f_c + \frac{Bt}{T} \quad (1)$$

where B is the signal bandwidth, T the sweep repetition time and f_c the carrier frequency. The corresponding phase is the integral with respect to time:

$$\mu(t) = 2\pi\left(f_c t + B\frac{t^2}{2T}\right) \quad (2)$$

Therefore we can write for the transmitted signal in the first sweep (defined by $n=0$)

$$v_x(t) = \cos\left(2\pi f_c t + \frac{\pi B t^2}{T}\right) \quad (3)$$

where we have omitted the amplitude for convenience. In the n^{th} sweep, (3) becomes

$$v_x(t) = \cos\left(2\pi f_c t + \frac{\pi B(t - nT)^2}{T}\right) \quad (4)$$

The returned voltage signal $v_r(t)$ leaves a target at distance R moving with radial velocity V at time $t = 0$. It has the same form as the transmitted signal but is multiplied by an amplitude factor which depends on distance as $1/R^2$ and is delayed in time by an amount given by

$$t_d = \frac{2(R + Vt)}{c} \quad (5)$$

So the return from the n^{th} sweep is given by

$$v_r(t) = \frac{1}{R^2} \cos\left(2\pi f_c [t - t_d] + \frac{\pi B(t - t_d - nT)^2}{T}\right) \quad (6)$$

Mixing of the returned and transmitted signals

The received signal is mixed with the transmitted signal to give

$$v_m(t) = v_r(t)v_x(t) \quad (7)$$

The mixed signal therefore contains the product of two cosine terms. Using the trigonometric identity $\cos A \cos B = (\cos(A-B) + \cos(A+B))/2$, we note that the sum term has a very high frequency (of order $2f_c$) which is filtered out, leaving the difference term:

$$v_m(t) = \frac{1}{R^2} \cos\left(\frac{4\pi f_c t_d}{c} + \frac{2\pi B t_d (t - nT) - \pi B t_d^2}{T}\right) \quad (8)$$

Substituting (5) into (8) gives

$$v_m(t) = \frac{1}{R^2} \cos\left(\frac{4\pi f_c (R+Vt)}{c} + \frac{4\pi B (R+Vt)(t - nT) - 4\pi B (R+Vt)^2}{cT}\right) \quad (9)$$

This mixed signal is to be processed to give estimates of the target range R and velocity V .

Processing the mixed signal

The optimum processing method is described by Barrick (1973). A fast Fourier

transform (FFT) is taken over each successive sweep, and the resulting transforms arranged as the rows of a matrix. A second set of FFTs is then taken over the columns of the matrix. We will now describe how range and velocity emerge from this process.

(a) FFTs over each sweep

Define t' to be the time from the start of the n^{th} sweep i. e.

$$t = nT + t' \quad (10)$$

Then, ignoring constant terms, which will merely change the absolute value of the phase, and terms quadratic in t'^2 , which are negligibly small for systems we will be considering, (9) can be written

$$v_m(t) = \frac{1}{R^2} \cos \left(2\pi \{ f_p t' + f_D T \} \right) \quad (11)$$

where we have defined two new terms, the peak frequency in the n^{th} sweep, f_p , and the Doppler shift, f_D , through the equations

$$f_D = \frac{2f_c V}{c} \quad (12)$$

$$f_p = \frac{2BR}{cT} + f_D + \frac{2BnV}{c} \quad (13)$$

We then take an M-point Fourier transform of the voltage time series of length T. For the n^{th} sweep, ignoring the effects of the finite length of the time series, this is given by

$$v_m^{\text{tr}}(f) = \frac{e^{2\pi i f_D n T}}{R^2} \delta[f - f_p] + \frac{e^{-2\pi i f_D n T}}{R^2} \delta[f + f_p] \quad (14)$$

where the superscript "tr" denotes the Fourier transform. Thus the spectrum contains two peaks at frequencies f_p and $-f_p$ with phases of equal magnitude and opposite sign. It can be seen from (13) that the peak frequency f_p depends on target position, velocity and sweep number; however, for cases we are considering, the last two terms will be

relatively small, so f_p is approximately constant from sweep to sweep and can be written

$$f_p \approx \frac{2BR}{cT} \quad (15)$$

However the phase associated with the peak is proportional to the sweep number ; it will be shown that this fact can be used to derive the target velocity through the second set of Fourier transforms. The range can then be determined from the peak frequency through (13).

In practice, one starts with M signal points in the time domain covering a single sweep with time resolution δt , so that

$$M \delta t = T. \quad (16)$$

Thus the time series is sampled at times

$$0, \delta t, 2\delta t, \dots, (M - 1)\delta t$$

After the FFT, one has spectral points at frequencies

$$-\frac{M}{2T}, \left(-\frac{M}{2} + 1\right)\frac{1}{T}, \dots, 0, \dots, \left(\frac{M}{2} - 1\right)\frac{1}{T}$$

From (15), these frequencies corresponds to range cells centered on

$$\frac{cM}{4B}, \frac{c}{2B}\left(\frac{M}{2} - 1\right), \dots, 0, \dots, \frac{c}{2B}\left(\frac{M}{2} - 1\right), \frac{cM}{4B}$$

where, for symmetry, we have repeated the ending range cell on the right. The resulting range resolution is given by:

$$\Delta R = \frac{c}{2B} \quad (17)$$

The number of terms M is defined in terms of the range window; if R_{\max} is the specified maximum range, M is defined by the relation

$$M = \frac{4BR_{\max}}{c} \quad (18)$$

From (15), the maximum baseband frequency f_B is given in terms of R_{\max} by

$$f_B = \frac{2BR_{\max}}{cT} \quad (19)$$

The time series is sampled at the Nyquist frequency, since from (16) and (18)

$$\delta t = \frac{cT}{4BR_{\max}} = \frac{1}{2f_B} \quad (20)$$

Note that the radar cannot detect targets beyond a limiting range R_{\lim} defined as the two-way distance traveled by the radar in a single sweep:

$$R_{\lim} = \frac{cT}{2} \quad (21)$$

At distances greater than R_{\lim} , targets at two different ranges can contribute to the spectrum at the same frequency, and there can be no unique determination of range. The sweep repetition periods considered here are sufficiently long that the range wrap-around due to this effect is not a problem.

(b) The second set of FFTs

The transforms over the pulses are then lined up in matrix form, successive rows corresponding to successive sweeps; the total number of sweeps, N , is dictated by the desired velocity resolution. This is demonstrated in (22); the index i indicates the sweep number.

	$f = -f_B$	\dots	$f = -f_p$	\dots	$f = f_p$	\dots	$f = f_B$
$i = 0$	0	0	$\frac{1}{R^2}$	\dots	$\frac{1}{R^2}$	0	0
$i = 1$	0	0	$\frac{e^{-2\pi i f_D T}}{R^2}$	\dots	$\frac{e^{2\pi i f_D T}}{R^2}$	0	0
\vdots	0	0	\vdots	\vdots	\vdots	0	0
$i = N$	0	0	$\frac{e^{-2\pi i N f_D T}}{R^2}$	\dots	$\frac{e^{2\pi i N f_D T}}{R^2}$	0	0

(22)

Thus with the neglect of the last term of (13), the columns of (22) consist of elements of constant amplitude and increasing phase which is proportional to the target Doppler shift f_D . This is easily derived by taking the Fourier transform of the columns, which are in effect N-point time series with sample interval equal to the sweep time T. The result of this transformation appears as follows:

	$f = -f_B$	\dots	$f = -f_p$	\dots	$f = f_p$	\dots	$f = f_B$
$f = -\frac{1}{2T}$	0	0	0	\dots	0	0	0
$f = -f_D$	0	0	$\frac{1}{R^2}$	\dots	0	0	0
\vdots	0	0	0	\vdots	0	0	0
$f = f_D$	0	0	\dots	\dots	$\frac{1}{R^2}$	0	0
$f = \frac{1}{2T}$	0	0	0	\dots	0	0	0

(23)

Thus there are two non-zero terms of equal amplitude at frequencies f_D and $-f_D$. Equation (23) is useful to illustrate the results; however it shows that the negative frequency spectral points from the first Fourier transform provide the same information as the positive. Therefore for efficiency only the positive frequencies are treated i.e. the right half of the columns of (22). The frequency resolution resulting from the second set of FFT's is given by $1/(NT)$ and, from (12) the resulting velocity resolution is therefore

$$\Delta V = \frac{c}{2NTf_c} \quad (24)$$

Accordingly, the number of sweeps must be adjusted to achieve a desired velocity resolution, using the relation

$$N = \frac{c}{2\Delta V T f_c} \quad (25)$$

To avoid aliasing, the sampling rate in the second set of FFT's must be equal or greater than the Nyquist rate given by:

$$T = \frac{c}{4f_c V_{\max}} \quad (26)$$

Thus the sweep repetition time is set by the maximum target velocity that is to be detected.

This signal processing scheme is optimum in the following sense: we started with a time series of NM points consisting of signal mixed with noise. After the processing, the signal power is confined to a narrow peak in frequency (ideally a delta function or, in practice, a single cell of the MxN range-Doppler space), while the noise is still spread across the entire band. This results in the maximum possible increase in signal-to noise ratio, i.e. the attributes of the "matched-filter" receiver.

Approximations

The simplified analysis described in this section contains several approximations which will now be summarized.

- (1) We have assumed the time series to be of infinite length when taking Fourier transforms.
- (2) The quadratic terms in the phase in (11) have been assumed negligible.
- (3) The target velocity has been assumed to be constant over the total coherent integration period.
- (4) The target velocity has been assumed to be small enough so that the peak frequency is the same from sweep to sweep i.e. we have neglected the last term in (13) for the peak frequency.

In the actual situation, the echo peaks, which in the idealized treatment are delta functions in frequency, will be somewhat displaced from their ideal positions, spread out in frequency, and reduced in amplitude. In Section 5, we examine the effect of these distortions on the accuracy of the derived target range and velocity.

SECTION 2: THE EFFECT OF GATING

In order to avoid saturation by the transmitted pulse, when the transmitter and receiver are colocated, the transmitter is turned off while the receiver is on with an approximate 50% duty factor. The inclusion of gating has two possible effects: (a) The creation of blind zones in the viewing area, i. e. regions of low signal strength (b) The creation of spurious echoes in addition to the main spectral peak.

Gate function in the time and frequency domain

The gating causes the received signal in the time domain to be multiplied by a repeated rectangular function (termed the gate function $G(t)$), that is defined by both the target range and the gate on-time, T_G . The effect of the gating on the signal is illustrated in Fig. 2. The transmitter and receiver signals are multiplied by the square-wave functions shown in Fig. 2(a), 2(b). The signal received at time t from a target at distance R was emitted at time $t-2R/c$. The delayed signal is shown in Fig 2(c). The received signal is multiplied by the product of (b) and (c), which defines the gate function to be a rectangle function of reduced width W equal to $2R/c$ for $2R/c < T_G$, as shown in Fig. 2(d). In a similar fashion, it may be shown that the product function over the complete range of distance R consists of rectangle functions of width W which can be written as a convolution

$$G(t) = \Pi\left(\frac{t}{W}\right) \otimes \sum_{i=0}^{\infty} \delta\left(t - (2i+1)T_G - \frac{R}{c}\right) \quad (27)$$

where \otimes denotes convolution and $\Pi(x)$ is the rectangle function defined by

$$\begin{aligned} \Pi(x) &= 1 & |x| \leq \frac{1}{2} \\ &= 0 & |x| > \frac{1}{2} \end{aligned}$$

The pulse width W depends on target range as the triangular function shown in Fig. 3, which defines regions of zero signal at ranges $0, cT_G, 2cT_G, \dots$

It is desirable to set the gate time T_G so that (i) there are no blind zones and (ii) the signal strength is maximum at the most distant range. It can be seen from Fig. 2 that this requires

$$T_G = \frac{2R_{\max}}{c} \quad (28)$$

The fact that the pulse width increases linearly with increasing range between 0 and R_{\max} tends to compensate for the previously noted $1/R^2$ decrease due to propagation loss: the gated signal strength now depends on the inversely on distance i.e. as $1/R$.

The Fourier transform of the gate function (27) is defined by

$$G^{\text{tr}}(f) = \frac{W \sin(\pi W f)}{(\pi W f)} \sum_{n=0}^{\infty} \delta\left(f - \frac{n}{2T_G}\right) \quad (29)$$

which describes a set of impulse functions at intervals of $1/(2T_G)$. The maximum value of $G^{\text{tr}}(f)$ is equal to W , i.e. the width of the step function shown in Fig. 3.

Spectrum of the gated signal

The Fourier transform of the gated signal is the convolution of (9) and (29). This convolution can give rise to spurious images after the first set of FFT's: for example a peak at frequency f_p will be associated with a spurious image at frequency f_p' with phase of opposite sign where

$$f_p' = \frac{1}{2T_G} - f_p \quad (30)$$

Spurious images will occur if f_p' falls within the baseband bandwidth $0 < f_p' < f_B$ or the following inequality is obeyed:

$$f_p > \left[\frac{1}{2T_G} - f_B \right] \quad (31)$$

The ratio, g , of the amplitude of the secondary peak to that of the primary is given by

$$g = \frac{\sin\left(\frac{\pi W}{2T_G}\right)}{\left(\frac{\pi W}{2T_G}\right)} \quad (32)$$

where W is the pulse width. Thus the amplitude of the secondary peak is always less than the primary. After the second set of Fourier transforms there will be two peaks at frequencies f_D and $-f_D$ with amplitudes in the ratio given by (21). The secondary peak therefore looks as if it were produced by a target moving in the opposite direction.

The formation of spurious images can be avoided by decreasing the gate on-time so that

$$T_G \leq \frac{1}{4f_B} \quad (33)$$

The two requirements on T_G , (19) and (33), for the removal of blind zones and spurious images can be mutually exclusive, depending on (i) the maximum target Doppler shift per range cell; (ii) the number of range gells required; and (iii) the maximum range.

SECTION 3: DESIGN OF A TRACKING SYSTEM

Specification of signal parameters

As described by Barrick (1973), these equations can be used to calculate signal parameters for a set of backscatter radar specifications. In this section, we will describe the design of a system for the detection of a discrete target moving at speeds of up to 300m/s. Assume that the following parameters are given:

- (1) The carrier frequency $f_c = 20$ MHz.
- (2) The maximum target range $R_{\max} = 48$ km.
- (3) The maximum target velocity $v_{\max} = 300$ m/s.
- (4) A range resolution of 3 km.
- (5) A velocity resolution of 1 m/s.

The following signal parameters may then be calculated.

- (1) The signal bandwidth $B = 50$ kHz (from equation 17)
- (2) The sweep repetition interval $T = 1/60$ s. (from equation 26)
- (3) The number of samples per sweep $M = 32$ (from equation 18)
- (4) The number of sweeps $N = 512$ (from equation 25)
- (5) The total time for a single coherent operation (i.e. MNT) is 8.5 s.

The bandpass filter after mixing is set to 1024 Hz. This removes high frequency noise which would be aliased down into the bandwidth of interest during the Fourier transform process and in addition removes the high frequency (second harmonic) term contained in (7).

Specification of gate period and duty factor

For a colocated transmitter and receiver, the receiver must be off when the transmitter is on; this means the duty factor must be less than or equal to 50%. The optimum signal to noise ratio is obtained therefore with the maximum value of 50%.

For the present example, the gate time T_G is chosen so there are no blind zones and the signal strength at the most distant ranges is maximized. From (28), this defines T_G to be 0.00032 s. With this gate period, it follows from (31) that spurious images will occur when the target is at ranges greater than 30 km.

SECTION 4: THE RADAR SIMULATOR

In this section we describe the simulation of radar echo spectra from realistic targets, using FMCW signals and the spectral processing described above. Figure 4 depicts the system operations modeled in the simulator. Gaussian zero-mean random noise is added to the received FMCW signal, which is then gated with a 50% duty factor. The noisy signal is then mixed to baseband, low-pass filtered and digitized. A Hamming window is then applied to the resulting signal which is double Fourier transformed, with output in digital form. The signal parameters used are given in the previous section.

Simulation of noise

In the ungated signal, the complex noise, n_f , at frequency f is assumed to be zero-mean, Gaussian, statistically independent from one frequency cell to another and flat, i.e. the average noise power is independent of frequency. Thus the real and imaginary components of the noise, n_{fr} and n_{fi} have zero mean and are uncorrelated with each other. The probability function can be written

$$p(n_{fr}) = \frac{1}{\sqrt{2\Pi}\sigma} e^{-\left(\frac{n_{fr}^2}{2\sigma^2}\right)} ; p(n_{fi}) = \frac{1}{\sqrt{2\Pi}\sigma} e^{-\left(\frac{n_{fi}^2}{2\sigma^2}\right)} \quad (34)$$

where the noise variance is σ^2 ; due to the gating, this variance is precisely one-half the average noise spectral power per frequency bin. In the gated signal, as described in Section 2, signal and noise in pairs of frequency bins (or range cells) are folded together by convolution. The noise n_f associated with frequency bin f before convolution is combined with that in frequency bin f' , $n_{f'}$, where f and f' are related by (30). The width of the pulse is always equal to the gate on-time T_G as the noise at the receiver is either on or off with a 50% duty factor; therefore the multiplicative factor for combining the noise is $2/\pi$ from (32). We can therefore write for the total noise at the two frequencies :

$$\dot{n}_f^{\text{total}} = \dot{n}_f + \frac{2}{\pi}\dot{n}_r \quad ; \quad \dot{n}_r^{\text{total}} = \dot{n}_r + \frac{2}{\pi}\dot{n}_f \quad (35)$$

In order to include the frequency cutoff at 1024 Hz due to the low-pass filter, to simulate realistic noise, random Gaussian noise samples for each sweep were generated in the frequency domain in the band 0-1024 Hz ; these uncorrelated samples were generated to have zero mean and a standard deviation set by the specified signal-to-noise ratio, which in turn was defined in terms of the weakest signal from the outermost range cell at 48 km. The noise spectrum for each sweep was then Fourier transformed to the time domain and added to the simulated FMCW received signal. The effect of gating with a 50% duty factor is to reduce the noise power by a factor of 2.

Example of a simulated spectrum

An example of a simulated spectrum is shown in Figure 5. A target at distance 30 km is approaching at a speed of 150 m/s. The signal to noise ratio is 10 at a the outer range of 48 km. Figure 5 shows the signal power plotted versus the frequencies of the two transforms of the double FFT process; thus Frequency 2 represents the actual Doppler shift of the target and Frequency 1 is given by (13) in terms of both range and velocity. The energy in the main peak at Frequency 1 equal to 20Hz is a factor of 40% larger than that in the spurious peak at -20Hz.

SECTION 5: INTERPRETATION OF THE SPECTRUM

In this section, we describe the processing required to interpret a measured spectrum which may contain several target echoes, to give their ranges and velocities. We first describe the identification of peaks in noise, then calculate the errors in range and velocity resulting from the approximations described in Section 3 and from additive Gaussian noise in the measurements, and finally discuss the problem of separating the spurious peaks arising from the signal gating. We make the following assumptions:

- (1) No two targets have the same range and velocity.
- (2) The signal-to-noise ratio (power) at the outer edge of the range window at 48 km exceeds 13 dB for the *ungated* signal. We shall treat the worst case, i.e. 13dB; it follows from equation (35) that the corresponding value for the gated signal is 11.5 dB, because the noise power increases by $1+(2/\pi)^2 = 1.5$ dB.

(a) *Identification of peaks*

An estimate of the noise power is made by averaging the right hand column after the first set of FFT's i.e. the spectrum for the outermost ranges which is least likely to contain signal power. After this initial averaging, spectral points exceeding three times this level are excluded and the remaining points averaged. This process removes the signal peaks and provides an estimate of the noise floor. Target echoes through the spectrum are then identified as those points that are 11.5 dB or more above this noise floor.

(b) *Calculation of target range and velocity*

The spectrum is analyzed using the double FFT method described in Section 1. In practice, the peaks that occur at a single frequency point in (23) are spread out both vertically and horizontally. The peak location in the spectrum is determined by finding the centroid in the horizontal and vertical directions before applying equations (12) and (13) to determine target range and velocity because of the approximations described in Section 1, the output includes bias error (i.e. the second and third terms of (13)) and because of noise in the data it also contains statistical error. Table 1 gives the bias errors for the example shown in Fig. 5, and Table 2 gives both bias and statistical errors calculated as a function of range and Doppler frequency. The magnitudes of these errors are less than 300m in range and 0.036Hz in Doppler (0.27m/s or .5 knot in velocity).

(c) *Identification of spurious echoes*

As described in Section 3, due to signal gating, a target at a range greater than 30 km

creates two echo peaks, the primary peak accompanied by a secondary peak that appears to have arisen from a target at different range and moving in the opposite direction. These peaks occur at paired frequencies related by (30). The spurious peak always has less energy than the primary and this fact can be used as the basis of a test to distinguish them. We will now derive the probability of error in the outcome of this test.

Let A_f be the complex voltage signal in the true range cell, where

$$\dot{A}_f = A_f \cos \phi + j A_f \sin \phi \quad (36)$$

where A_f is the amplitude and ϕ is the phase. Then the spurious signal at frequency f' is equal to

$$\dot{A}_{f'} = g \dot{A}_f \quad (37)$$

where the factor g is given by (32). We define a test function Q as the difference between the power in the two peaks; if the secondary is subtracted from the primary, this is given by:

$$Q = |\dot{A}_f|^2 (1 - g^2) \quad (38)$$

The test is based on the sign of Q ; e.g. if Q is positive the first peak is taken to be the primary. The probability of Q being greater than zero in the presence of noise can be written:

$$\text{Prob}(Q > 0) = \frac{1}{\sqrt{2\pi}\epsilon} \int_{-A^2(1-g^2)}^{\infty} e^{-\frac{\xi^2}{2\epsilon^2}} d\xi = \frac{1}{2} \left\{ 1 + \text{erf} \left(\frac{A_f^2 [1-g^2]}{\sqrt{2}\epsilon} \right) \right\} \quad (39)$$

where ξ represents the noise in the test function which is Gaussian random noise of

zero mean and variance ε^2 given in terms of the noise power σ^2 by

$$\varepsilon^2 = 4 \left[\left(1 - \frac{2g}{\pi}\right)^2 + \left(\frac{2}{\pi} - g\right)^2 \right] \sigma^2 \quad (40)$$

Substituting (36) into (39), expanding and including only first order terms in the small noise approximation, (39) can be written

$$\begin{aligned} Q &= A_f^2(1 - g^2) + 2A_f \left\{ \left(1 - \frac{2g}{\pi}\right) (\cos\phi_{n_{fr}} + \sin\phi_{n_{fi}}) + \left(\frac{2}{\pi} - g\right) (\cos\phi_{n_{fr}} + \sin\phi_{n_{fi}}) \right\} \\ &= A_f^2(1 - g^2) + \xi \end{aligned} \quad (41)$$

The probability of success in distinguishing the primary peak is then the probability that the test function Q is greater than zero, or

$$\text{Prob}(Q > 0) \text{ or } \text{Prob}(\xi > -A_f^2(1 - g^2)) \quad (42)$$

This probability can be written in integral form

$$\text{Prob}(Q > 0) = \frac{1}{\sqrt{2\pi\varepsilon}} \int_{-A_f^2(1-g^2)}^{\infty} e^{-\frac{\xi^2}{2\varepsilon^2}} d\xi = \frac{1}{2} \left\{ 1 + \text{erf} \left(\frac{A_f^2 [1-g^2]}{\sqrt{2\varepsilon}} \right) \right\} \quad (43)$$

Figure 6 shows this probability function plotted versus range, for a value of the signal-to-noise ratio at the outer range equal to 13 dB, and using the fact that A_f depends on range as $1/R$. The probability function shown in Fig. 6 represents the worst possible case; the actual probability of success is always greater than this for situations we are considering. Further, the amplitude of both peaks depends on target distance as $1/R$,

thus if the target is approaching/receding the peaks will increase/decrease with time, which can also be used as a distinguishing factor. We therefore conclude that we can distinguish the spurious peak with a high degree of certainty.

CONCLUSION

We have described the principles of FMCW signal processing for a gated signal and backed it up with an example of hard target detection. The resulting signal-to-noise ratio is considerably enhanced over the conventional pulse radar, due to the extended time the system is on. The same analysis methods apply to the optimum processing of signals that extend over a frequency range, for example sea echo.

REFERENCE

Barrick D. E. (1973): "FM/CW Radar Signals and Digital Processing", NOAA Technical Report ERL 283-WPL 26

APPENDIX

Definition of symbols used, in alphabetical order.

A_f	Complex voltage at frequency f
A_f	Amplitude at frequency f
B	Signal bandwidth
c	Velocity of light
f	frequency
f'	Frequency of spurious peak associated with a primary peak at frequency f
f_B	Maximum baseband frequency
f_c	Carrier frequency
f_D	Doppler shift
f_p	Peak frequency in the n^{th} sweep
g	Ratio of amplitude of the secondary to the primary peak
$G(t)$	Gate function multiplying the received signal
M	Number of points in the first set of FFTs
N	Total number of sweeps in a single coherent operation
n	Sweep number
n_f	Complex noise voltage at frequency f (ungated signal)
n_f^{total}	Complex noise voltage at frequency f (gated signal)
n_{fr}	Real component of n_f
n_{fi}	Imaginary component of n_f
Q	Test function for distinguishing the spurious peak from the primary
R	Range
R_{max}	Maximum range
R_{lim}	Limiting range set by the sweep period
t	time
t'	Time from start of the n^{th} sweep

t_D	Time delay
tr	Fourier transform
T	Sweep repetition period
T_G	Gate period
V	velocity
$v_m(t)$	Mixed signal voltage
$v_x(t)$	Transmitted signal voltage
$v_r(t)$	Received signal voltage
W	Width of received pulse
ε^2	Variance of the noise in the test function P
ϕ	Phase of ungated spectrum at frequency f
$\mu(t)$	Phase of transmitted signal at time t
ΔR	Range resolution
ΔV	Velocity resolution
δt	Time resolution
$\Pi(x)$	Rectangle function
σ^2	Noise variance in the spectrum of the ungated signal
ξ	Random noise in the test function P

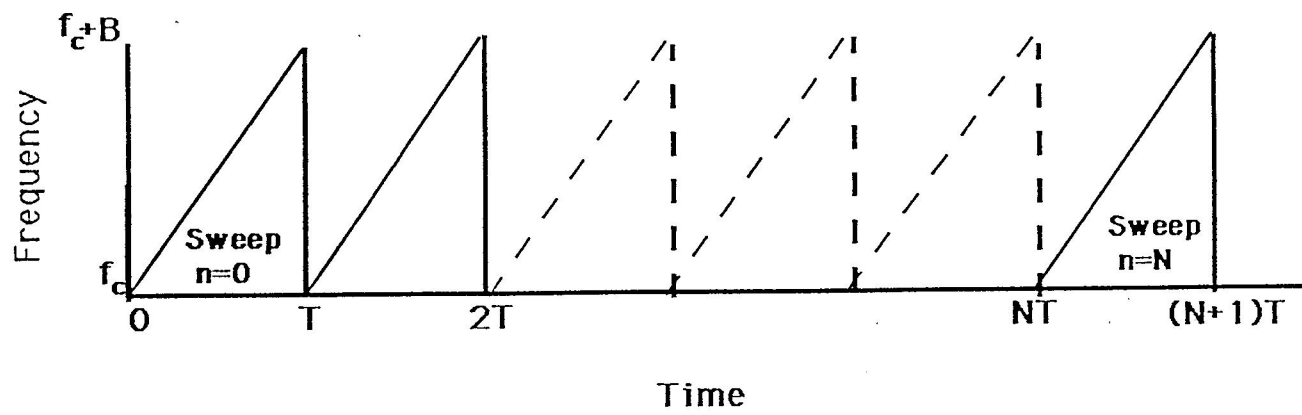


Figure 1

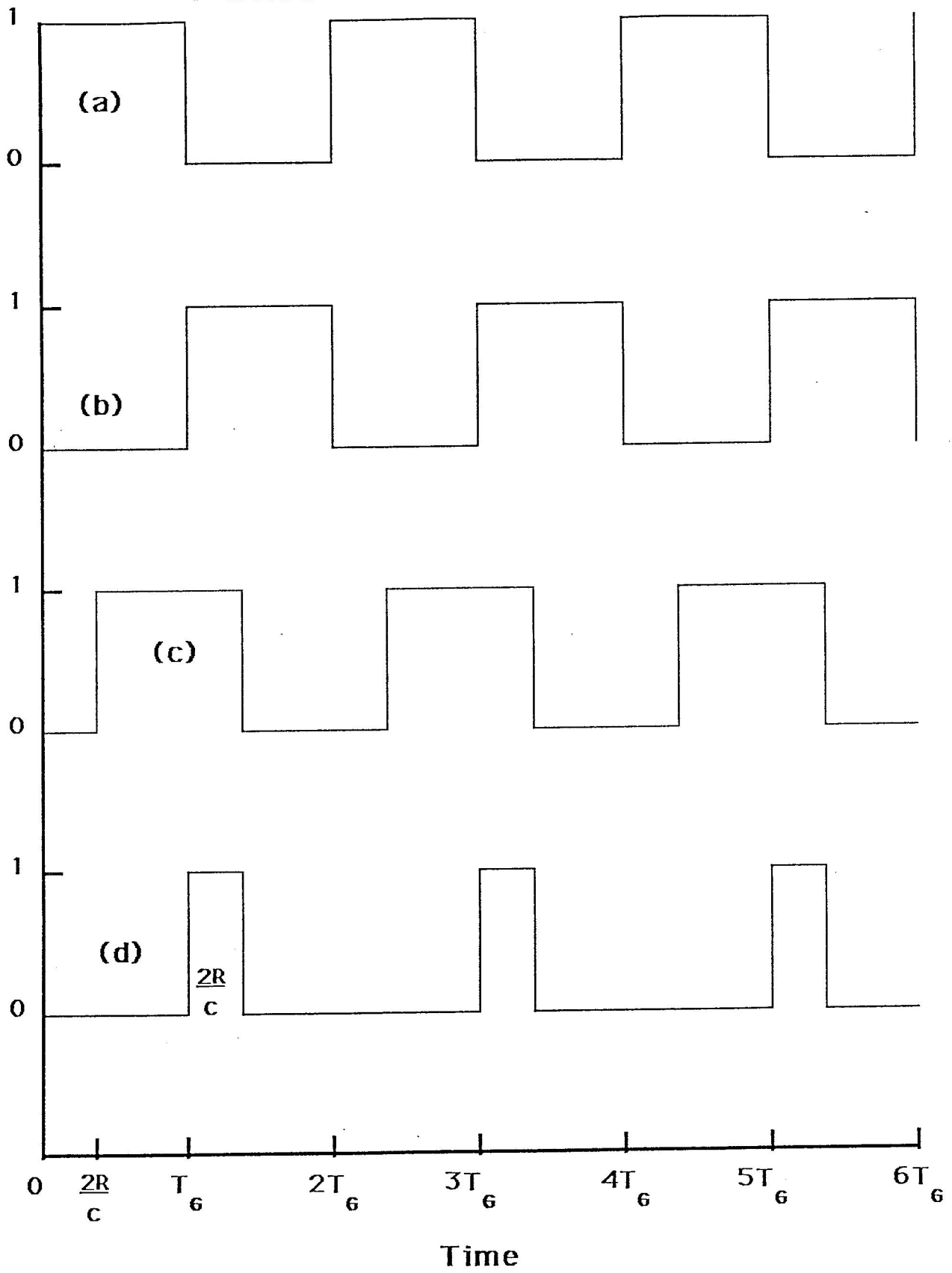


Figure 2

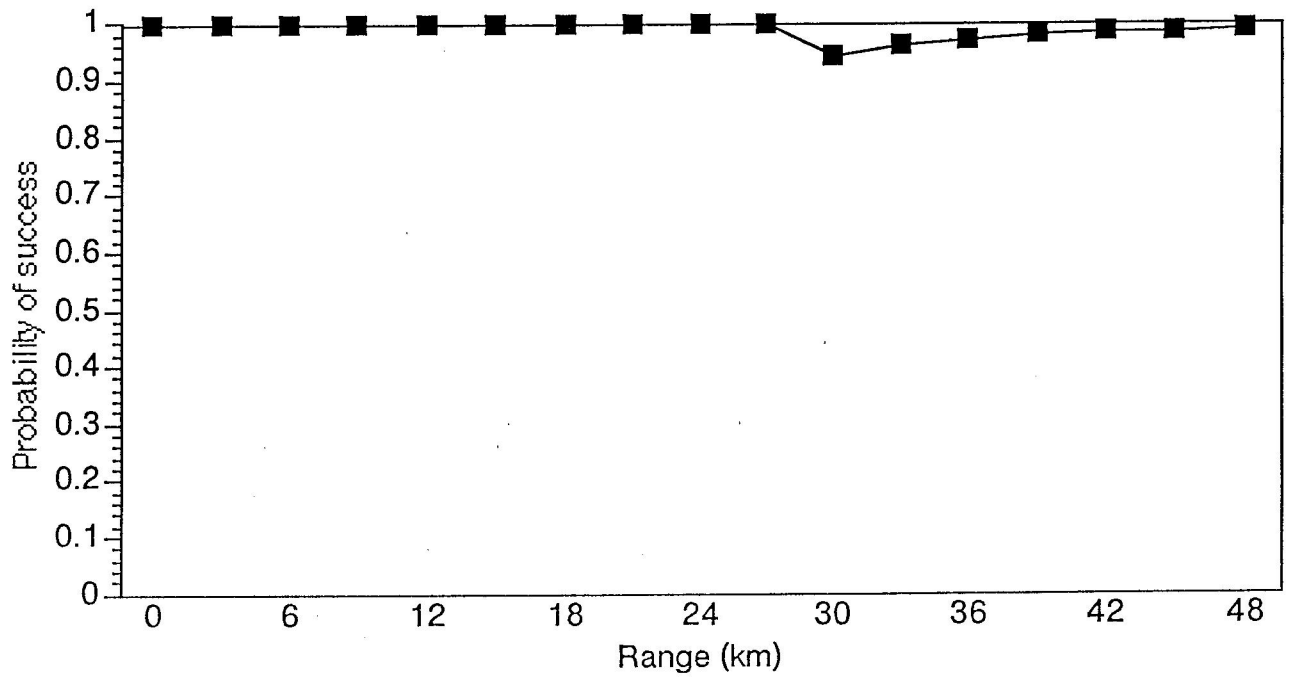
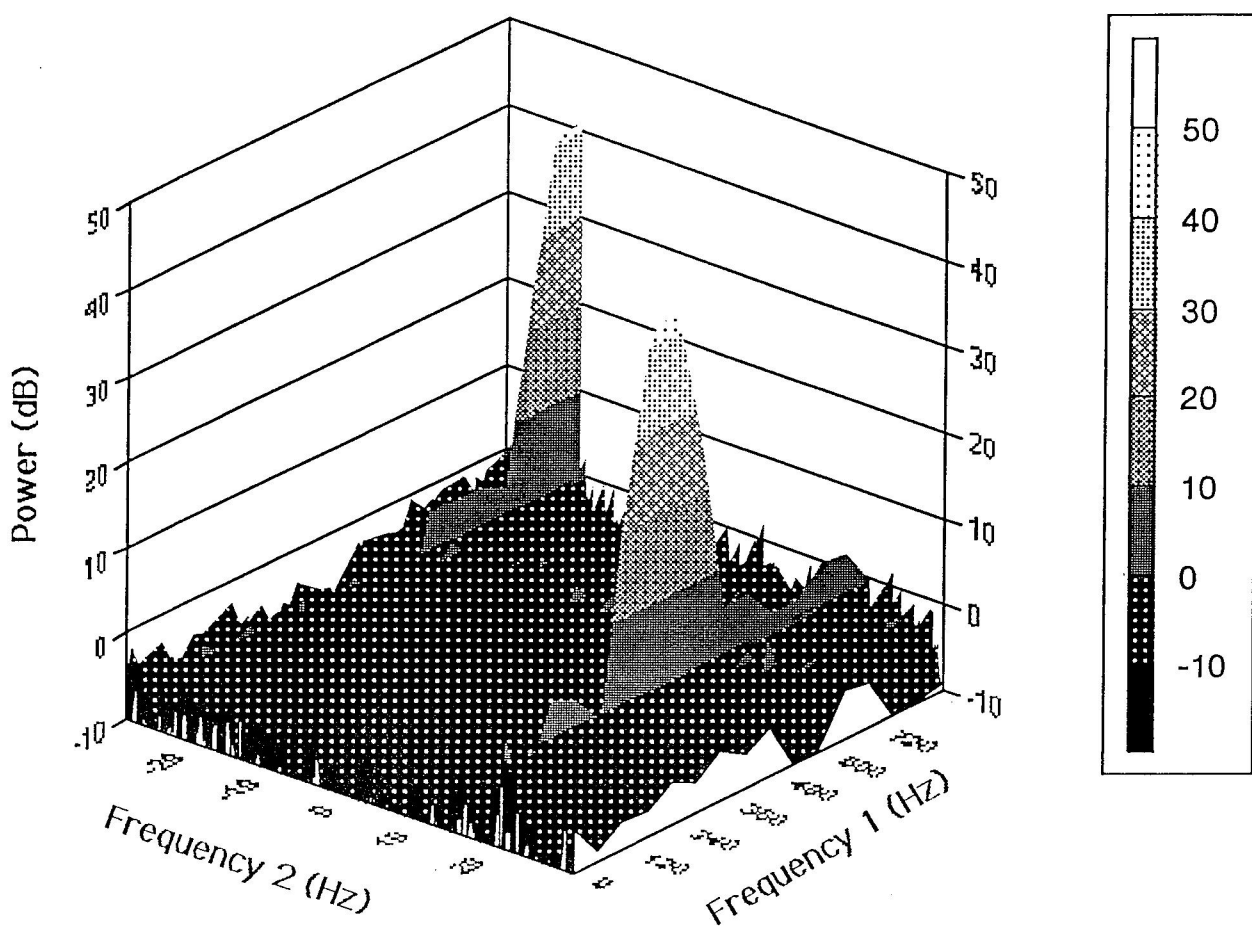


Figure 6



$S / N = 10$

Figure 5

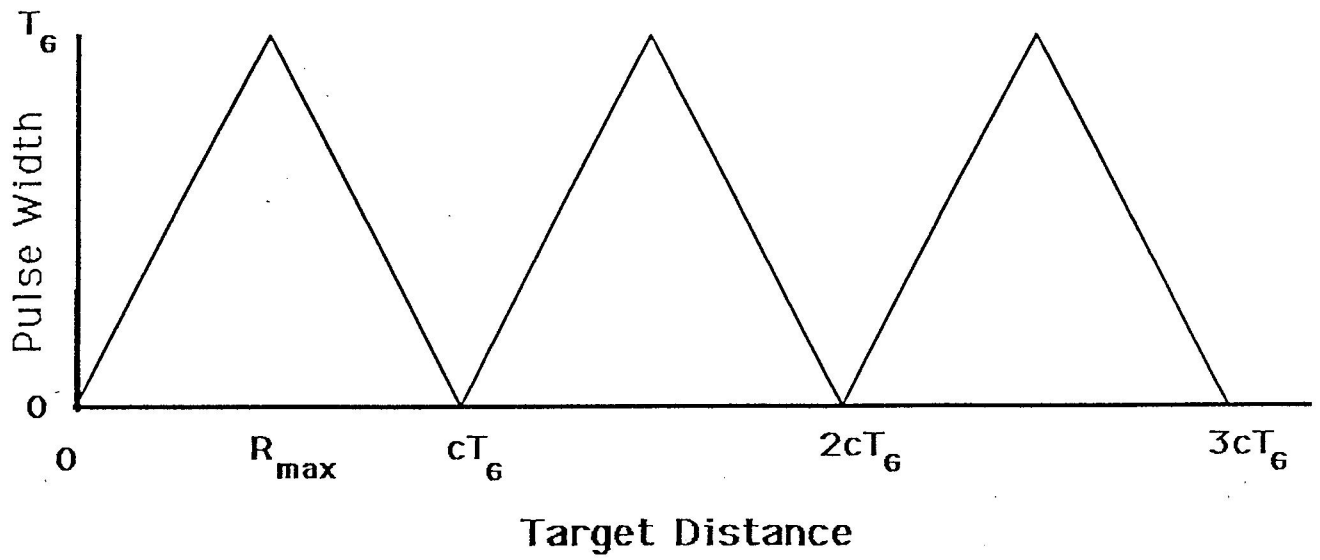


Figure 3

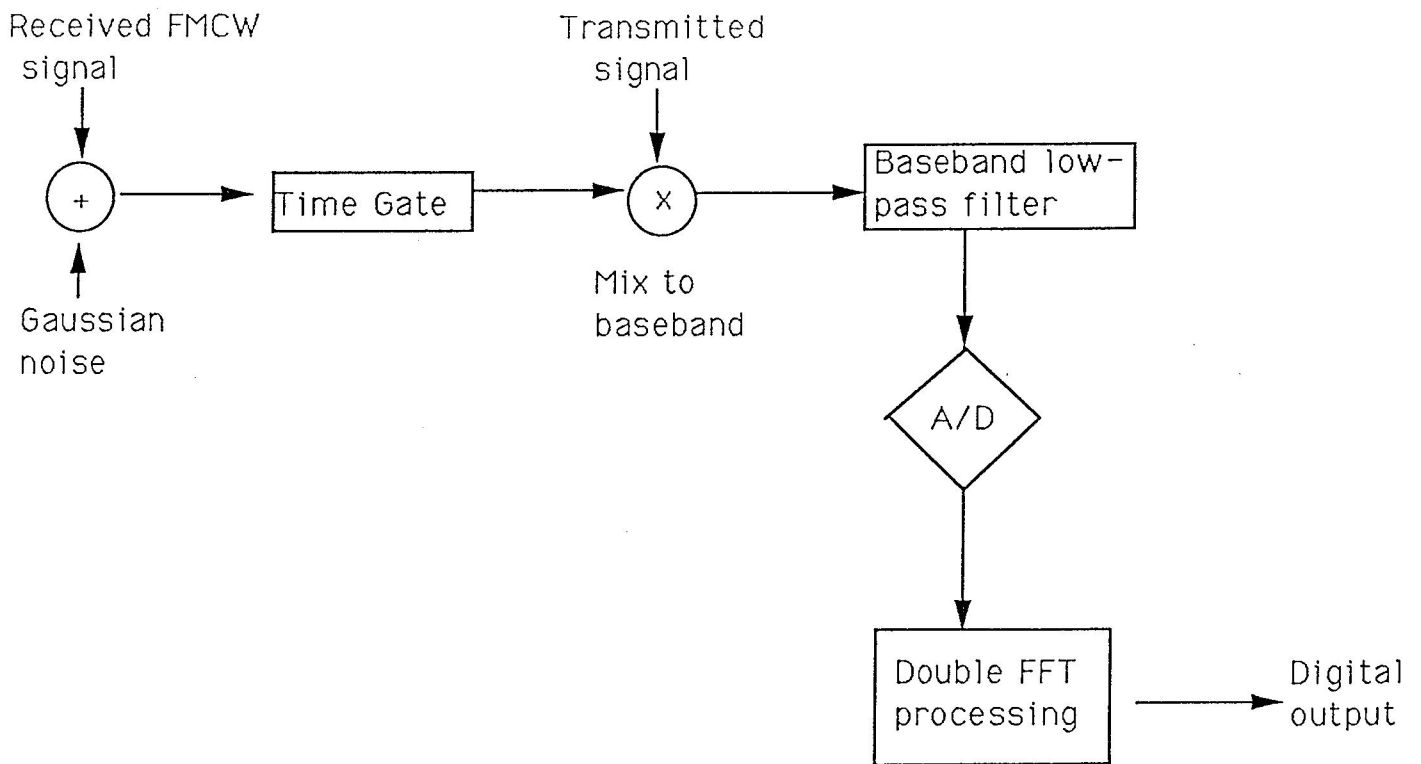


Figure 4